Characterization of the causality between spike trains with permutation conditional mutual information

Zhaohui Li, Gaoxiang Ouyang, Duan Li, and Xiaoli Li

Phys. Rev. E **84**, 021929 — Published 25 August 2011

DOI: 10.1103/PhysRevE.84.021929

Characterization of the causality between spike trains with permutation conditional mutual information

Zhaohui Li[1], Gaoxiang Ouyang[2], Duan Li[1], Xiaoli Li[2,3,*]

[1]*Institute of Information Science and Engineering, Yanshan University, Qinhuangdao 066004, People's Republic of China*

[2]*Institute of Electrical Engineering, Yanshan University, Qinhuangdao 066004, People's Republic of China*

[3]*National Key Laboratory of Cognitive Neuroscience and Learning, Beijing Normal Univeristy, Beijing, 100088, People's Republic of China*

Abstract

Uncovering the causal relationship between spike train recordings from different neurons is a key issue for understanding the neural coding. This study presents a method, called as permutation conditional mutual information (PCMI), for characterizing the causality between a pair of neurons. The performance of this method is demonstrated with the spike trains generated by Poisson point process model and Izhikevich's neuronal model, including estimation of the directionality index and detection of the temporal dynamics of the causal link. Simulations show that the PCMI method is superior to the transfer entropy and causal entropy methods at identifying the coupling direction between the spike trains. The advantages of PCMI include twofold: it is able to estimate the directionality index under the weak coupling and against the missing and extra spikes.

PACS: 87.19.La; 87.80.Tq.

[*]Corresponding author: xlli@ysu.edu.cn

I. INTRODUCTION

Over the past decades, most studies by means of spike trains have focused on the understanding of the neural coding [1-4]. It is of great interest to find out how neurons process and transmit information, which is a foundational issue for understanding the function of neuronal circuits and systems [5, 6]. To this end, simultaneously recording of multiple single neurons was employed, including multielectrode arrays [7, 8], multiple single electrodes [9] and optical imaging [10-12] et al.. By using the recorded spike trains, it is possible to study the interaction among neurons and their relationships within neural systems and then quantify the neural network's structural information to investigate the neural coding. Analysis of spike trains can give functional information such as the coupling strength and direction [5, 6, 13, 14].

Most analytical methods concentrate on the strength of pairwise connections, i.e. the degree of similarity or dissimilarity between two spike trains, including the cost-based metric [15, 16], the van Rossum distance [17], correlation based methods [18, 19], event synchronization method [20] and the ISI distance [21]. These methods have been successfully used to find the temporal similar pattern of the spike trains [22-24]. However, above methods are symmetric, and thus they can't capture the causal relationship between spike trains. To obtain the causal relationship between the spike trains, Granger causality and information-theory based causality were proposed. Granger causality method evaluates the coupling directions by determining whether the information of a neuronal series is useful in forecasting [25-30]. In recent years, Granger causality has been used to estimate the coupling direction in spike trains [31, 32]. But it has two disadvantages: requirement of stationarity and reliance on second-order statistics [31]. Another method for estimating the causality between neural series based on the information theory, such as conditional mutual information [33, 34], transfer entropy [35, 36], and permutation entropy [37, 38]. The details on these methods can be found in Ref. [39]. At present, to estimate the causality between two spike trains, two main methods: causal entropy [40] and transfer entropy [41], were applied. The causal entropy (CE) is a time-adaptive approach to detect the asymmetries in the relative inter-spike intervals between neuronal pairs. The transfer entropy (TE) quantifies the fraction of information in the past of a neuron flowed to the future of another neuron.

In this study, we address an information-theory based approach, which is referred as permutation conditional mutual information (PCMI), to extract the causality between spike trains recorded from a pair of neurons. The permutation entropy and conditional mutual information have been used to analyze neural signals [42-46]. Recently, the two methods have been integrated together, named as PCMI, to evaluate the directionality index between two cardiorespiratory series [47] and to estimate the coupling direction between two neuronal populations [48]. In this study, we intend to estimate the coupling direction between the spike trains by means of PCMI. The performance of the approach is evaluated using a Poisson process model by comparing with the TE and CE method.

II. METHODS

A. Transfer entropy (TE)

The transfer entropy can estimate the information transferred from one neuron to another neuron [41]. Let $[t \;\; t+\tau_f]$ and $[t-\tau_p \;\; t]$ denote the upcoming time interval and past time interval, respectively, and X^F, X^P and Y^F, Y^P are the number of spikes of S_X and S_Y (S_X and S_Y denote two spike trains) falling in the two intervals, then the transfer entropy from S_X to S_Y is defined as:

$$\varphi_{X\to Y} = I\left(Y^F; X^P \mid Y^P\right) = H\left(Y^F \mid Y^P\right) - H\left(Y^F \mid X^P, Y^P\right). \tag{1}$$

To reduce the bias caused by the surrogate data that generated by randomly shuffling the inter-spike intervals, the normalized transfer entropy (NTE) is defined as:

$$\psi_{X\to Y} = \frac{\varphi_{X\to Y} - \varphi_{X\to Y}^{\text{shuffled}}}{H\left(Y^F \mid Y^P\right)}. \tag{2}$$

There is no causality between two spike trains, when the NTE is less than zero. To restrict the NTE in the interval [0 1], we set up: $\psi = 0$ if $\psi < 0$. The directionality index $D_{X\to Y}^T$ (D^T: the directionality index of TE) is defined as:

$$D_{X\to Y}^{T}=\left(\frac{\psi_{X\to Y}-\psi_{Y\to X}}{\psi_{X\to Y}+\psi_{Y\to X}}\right)\in[-1\ 1], \tag{3}$$

The $D_{X\to Y}^{T}$ is greater than 0 if the spike train S_X drive the spike train S_Y; if the $D_{X\to Y}^{T}$ is less than 0 that means the spike train S_X is driven by the spike train S_Y; if the $D_{X\to Y}^{T}$ is about 0, there is no causal relationship between the two spike trains.

B. Causal entropy (CE)

The causal entropy is an information-theory method to estimate the causal relationship between two spike trains [40, 49]. The method is based on the variations of the distribution of inter-spike intervals in S_X and S_Y. The detail of the algorithm can be found in Ref. [40]. Herein the $\xi_{X\to Y}$ and $\xi_{Y\to X}$ are denoted as the causal entropies between S_X and S_Y. The normalized directionality index of CE is defined as:

$$D_{X\to Y}^{C}=-\frac{\xi_{X\to Y}-\xi_{Y\to X}}{\xi_{X\to Y}+\xi_{Y\to X}}\in[-1\ 1]. \tag{4}$$

where $D_{X\to Y}^{C}$ (D^{C}: the directionality index of CE) has the same meaning as the $D_{X\to Y}^{T}$.

C. Permutation conditional mutual information (PCMI)

The spike trains are series of the occurrence of action potentials recorded from individual neurons, each spike train can then be represented as a series of impulse functions:

$$S(t)=\sum_{i=1}^{W}\delta(t-t_i) \tag{5}$$

where $t_1\cdots t_W$ are the spike times and W denotes the number of spikes. In order to analyze with PCMI, a temporal resolution Δ (i.e. the bin size) is employed to discretize a spike train to a sequence of integers $N=\{N_1,N_2,\cdots,N_n\}$ [50, 51], where each integer N_i ($i=1,2,\cdots,n$, $n=T/\Delta$ is the total number of time steps within the

recorded time interval of length T) denotes the number of spikes occurred in each bin. The scheme is illustrated in Fig. 1(a) and 1(b). Less spikes will fall into a bin with the decrease of bins. If Δ is equal to the sampling period of the spike train, the sequence will become a binary one.

Like EEG (electroencephalogram) and LFP (local filed potential), the discretized spike trains may generally present as a fluctuation over time. The motifs (i.e. ordinal patterns, defined in Ref. [38] and denoted as M in this study) embedded in the fluctuations may provide the causal information between two spike trains. According to the definition of permutation entropy [37], the number of total motifs is equal to the factorial of the order (i.e. the number of data points in each motif). For example, there are six different motifs when order $m=3$, including 'slopes', 'peaks' and 'troughs', which are illustrated in Fig. 1(c). The order m is an important parameter in the PCMI algorithm, and how to choose its value will be discussed in the following section. It should be noted that there is a little difference in the sorting method in discretized spike trains compared with the method in EEG or LFP. The values in the fragment of continuous EEG or LFP signal have a continuous distribution, equal values are neglected and only unequal ones are considered for simplicity [37]. However, in the discretized spike trains, the equal values can't be simply neglected. Otherwise the temporal patterns contained in spike trains will be destroyed severely by the removal of equal values. To solve this problem, the approach employed in this study contains the following step: two equal values for sorting $N_i = N_j$, $i < j$, are treated as $N_i < N_j$, i.e. a ascending pattern. As shown in Fig. 1(c), the ordinal pattern that is composed of three data points denoted as solid triangles is classified as M_5.

Another important parameter is the lag τ in PCMI. The lag is the number of sample points spanned by each section of the motif [38]. The motifs under $\tau = 1$ and $\tau = 2$ are illustrated in Fig. 1(c). The motifs inside the ellipses are of lag $\tau = 1$ and the motif indicated by the solid squares is of lag $\tau = 2$. The effect of lag τ on the result of PCMI in the discretized spike trains will be addressed in the following section. Now, the probability of occurrence of each motif can be calculated as $p(M_i) = f(M_i) \big/ \left(n-(m-1)\tau\right)$, where $f(M_i)$, $i \in (1:m!)$ denotes the frequency of M_i in the discretized spike trains, n is the length of the discretized spike trains.

On the basis of the permutation analysis, the probability distribution functions, the joint probability functions and the conditional probability functions of two discretized spike trains can be obtained, and then the conditional mutual information can be calculated. Let S_X and S_Y be two spike trains recorded from two neurons. Their corresponding discretized sequences are $X=\{x_n\}$ and $Y=\{y_n\}$, respectively. The marginal probability distribution functions of *X* and *Y* are denoted as $p(x)$ and $p(y)$, respectively; the joint probability function of *X* and *Y* is denoted as $p(x,y)$. Then, the entropy of *X* and *Y* can be defined as [52]:

$$H(X)=-\sum_{x\in X} p(x)\log p(x), \tag{6}$$

and

$$H(Y)=-\sum_{y\in Y} p(y)\log p(y). \tag{7}$$

The joint entropy $H(X,Y)$ of *X* and *Y* is given by

$$H(X,Y)=-\sum_{x\in X}\sum_{y\in Y} p(x,y)\log p(x,y). \tag{8}$$

The conditional entropy $H(X\mid Y)$ of *X* given *Y* is defined as

$$H(X\mid Y)=-\sum_{x\in X}\sum_{y\in Y} p(x,y)\log p(x\mid y). \tag{9}$$

Then, the common information contained in both *X* and *Y* can be evaluated by the mutual information:

$$I(X;Y)=H(X)+H(Y)-H(X,Y). \tag{10}$$

To infer the causal relationship, i.e., the directionality of the coupling between *X* and *Y*, the conditional mutual information (CMI, i.e. the PCMI in this study) may be employed to estimate the “net” information about the future of one process contained within the other process. The PCMI between *X* and *Y* can be calculated by the following equations [33, 34, 48]:

$$I_{X\to Y}^{\delta}=I\left(X;Y_{\delta}\mid Y\right)=H\left(X\mid Y\right)+H\left(Y_{\delta}\mid Y\right)-H\left(X,Y_{\delta}\mid Y\right) \tag{11}$$

and

$$I_{Y\to X}^{\delta}=I\left(Y;X_{\delta}\mid X\right)=H\left(Y\mid X\right)+H\left(X_{\delta}\mid X\right)-H\left(Y,X_{\delta}\mid X\right), \tag{12}$$

where $X_{\delta}(Y_{\delta})$ is the future δ steps ahead of the process $X(Y)$. The main procedure of the algorithm to detect the coupling direction is as follows:

(1) Find the maximum value in $I_{X\to Y}^{\delta}$ and $I_{Y\to X}^{\delta}$, then denoted as $I_{X\to Y}^{\eta}$ and $I_{Y\to X}^{\eta}$;

(2) Similarly to Refs. [53, 54], the directionality index between X and Y is defined as:

$$D_{X\to Y}^{P}=\left(\frac{I_{X\to Y}^{\eta}-I_{Y\to X}^{\eta}}{I_{X\to Y}^{\eta}+I_{Y\to X}^{\eta}}\right). \tag{13}$$

Since both $I_{X\to Y}^{\eta}$ and $I_{Y\to X}^{\eta}$ are confined in the interval [0 1], the value of $D_{X\to Y}^{P}$ (D^{P}: the directionality index of PCMI) ranges from -1 to 1. $D_{X\to Y}^{P}>0$ means that S_X drives S_Y and $D_{X\to Y}^{P}<0$ means that S_Y drives S_X. The matlab codes for the algorithm are available online [55].

III. SIMULATION AND RESULTS

A. Models for spike trains

In this study, to evaluate the performance of the proposed method, Poisson point process model and Izhikevich's neuronal model are employed for the simulation analysis. The underlying idea of Poisson point process model is that the inter-spike intervals within a spike train follow a Poisson distribution, it was known that the Poisson-like spike trains are the fundamental unit of cortical communication[56, 57]. On the other hand, the Izhikevich's neuronal model combines the biological plausibility of Hodgkin-Huxley-type dynamics and the computational efficiency of integrate-and-fire neurons, this simple model can generate the rich behavior of biological neurons, including spiking, bursting, and mixed mode firing patters[58].

(1) Poisson point process model

Poisson point processes have been employed to generate spike trains for simulation studies [17, 59, 60]. The processing for generating a Poisson spike train is that each successive spike time is the previous spike time plus an inter-spike interval which is randomly picked up from an exponential distribution. In order to investigate the interaction between two spike trains, we set up a causality link for the two spike trains by the method proposed in Ref. [41], as shown in Fig. 2. The detail is below. Firstly, two independent Poisson processes are used to simulate two spike trains S_X and S_Y with firing rates of λ ($\lambda = 10$ Hz is chosen in this study which means 10 spikes/s); Secondly, a proportion $\alpha \in [0\ 1]$ of spikes in the S_Y are removed, the number is denoted as L; Lastly, the spike trains of L are picked up randomly from the S_X and are inserted into the S_Y with a delay time (denoted as 'd_P' in the following sections) to generate a new spike train. Through this transform, the S_Y spike train will contain the causal information from the S_X spike trains. The causal information between the spike trains S_X and S_Y is proportional to α.

(2) Izhikevich's neuronal model

The Izhikevich neuronal model contains two variables [58]: v and u, v is the membrane potential of the neuron and u is a membrane recovery variable, the model is below

$$v' = 0.04v^2 + 5v + 140 - u + I, \tag{13}$$

$$u' = a(bv - u). \tag{14}$$

with the auxiliary after-spike resetting

$$if\ v \geq 30mv, then \begin{cases} v \leftarrow c \\ u \leftarrow u + d. \end{cases} \tag{15}$$

where I is the synaptic current or injected DC current. The parameter a describes the time scale of u, b describes the sensitivity of u to subthreshold fluctuations in v, c describes the spike reset values of v and d describes the spike reset value of u. These parameters are set as: $a = 0.02, b = 0.2, c = -65mv, d = 2$.The injected current I is set as a normally distributed random Gaussian variable. The causality between two neurons is obtained in such a way: the output of the first neuron is fed into the second

neuron with time delay (denoted as 'd_1' in the following sections), as shown in Fig. 3. The coupling strength is determined by a proportion *R* which means how many percents of the output of neuron 1 are injected into neuron 2. The larger is the proportion, the stronger coupling between the two neurons.

B. Parameter choices in PCMI

In the PCMI algorithm, four different parameters (i.e. Δ, τ, *order* and δ) should be firstly considered before its application. The effect of these parameters selections on the performance of the PCMI is discussed by the Poisson point process model, the similar results can be found from the Izhikevich neuronal model. Given $\alpha = 0.5$, $d_P = 25\text{ms}$, and the spike train length 50s, two spike trains are generated.

(1) The temporal resolution Δ. The Δ is the bin size that is used to discretize spike trains. The Δ ranges from 1ms to 30ms with a step of 1ms. Fig. 4 plots the directionality index estimated by the PCMI with order $m = 2$ and $m = 3$, respectively. For $m = 2$, it can estimate the coupling direction when $\Delta < 15\text{ms}$; while $m = 3$, when Δ is larger than 10ms, the coupling direction cannot be found. The underlying reason is that the larger Δ destroy the inherent permutation patterns contained in the two spike trains, however the smaller the Δ, the more accurate permutation information can be obtained. In this study, it is recommended that the Δ is set as the sample period of the spike train, namely $\Delta = 1\text{ms}$.

(2) The lag τ. The lag is the number of data points between the adjacent two points in the motifs. Fig. 5 shows the directionality index at the different lags with $m = 2$ and $m = 3$, it is found that the different lags can give similar results for the two orders. In [61], an autocorrelation function (ACF) of a signal can be employed to determine the lag τ. In this study, we found the lag τ determined by the ACF is always one, so the $\tau = 1$ is selected in this simulation analysis.

(3) The order *m*. The order denotes the number of data points included in the motif. The length of data is at least greater than $m! * m! * m!$ points to obtain a reliable result of PCMI, for example $m = 4$ means we need 13824 data points [48]. In this study, there are only 0s and 1s in the binary sequences, when $m = 2$

(ascending and descending ordinal patterns), the permutation patterns of the series can be fully described. As can be seen in Fig. 4 and Fig. 5, $m = 2$ is an appropriate selection for the calculation of PCMI.

(4) The δ. It is noted that the δ cannot be less than the order *m* in PCMI [47]. And the δ is associated with the delay time, which will be discussed in the following section. Thus, the δ should be larger than the maximal delay between two spike trains for investigating the causality at all delay times.

C. Simulation results

Firstly, the capability of PCMI for charactering the causal relationship is demonstrated by the mentioned two models. In the Poisson point process model, model P_1 and model P_2 are constructed and shown in Fig. 6(a) and 6(b), respectively. In model P_1, $\alpha = 0.5$ and $d_P = 15\text{ms}$, two spike trains S_X and S_Y of 10s are generated with the causality from S_X to S_Y. In model P_2, the coupling direction is the same as model P_1 but the strength is composed of three fractions: $\alpha_1 = 0.15$ with $d_P^1 = 10\text{ms}$, $\alpha_2 = 0.2$ with $d_P^2 = 20\text{ms}$ and $\alpha_3 = 0.15$ with $d_P^3 = 30\text{ms}$. The reason for the usage of the model P_2 is that the coupling between neurons may involve multiple pathways that vary in their conduction delays [62]. For both models, we use $\Delta = 1\text{ms}$ to discretize the two spike trains and $m = 2$, $\tau = 1$, $\delta = 2:50$ to calculate the PCMI. Fig. 6(c) and 6(d) plot the PCMI values between S_X and S_Y ($I_{X\to Y}$ and $I_{Y\to X}$) with different δ values for model P_1 and model P_2, respectively. Obviously, there is a peak of $I_{X\to Y}$ corresponding to every delay time in the two models, which is indicated by the product of δ and Δ (e.g. $\delta = 15$ and $\Delta = 1\text{ms}$ for 15ms delay). In fact, Δ identifies the resolution of the delay times. Moreover, the value of $I_{X\to Y}$ is proportional to the coupling strength, as can be observed in Fig. 6(d). On the other hand, the $I_{Y\to X}$ stays closely to 0 due to the absence of causality from S_Y to S_X. The estimated directionality indexes for the two models, 0.98 and 0.96 respectively, reflect the coupling direction exactly.

In the Izhikevich's neuronal model, model I_1 and model I_2 are constructed and shown in Fig. 7(a) and 7(b). As can be seen in Fig. 7(c) and 7(d), the causal relationship between neurons can be revealed by the simulation results. The details on the simulation are similar to ones of the Poisson point process model. Thus, the PCMI

method can give not only the coupling strength, but also the causality between two neurons.

Secondly, to compare with the PCMI, the TE and CE methods are carried out with the same simulations. As mentioned in the previous section, the PCMI, TE, and CE are all parameter-dependent methods. We set the parameters of the three methods as follows: $\delta = 2:50$ for PCMI; $\tau_f = 1:50\text{ms}$ and $\tau_p = 1:50\text{ms}$ for TE; 10 bins of size 5ms for CE. The comparison is carried out in three aspects.

(1) Variation of directionality index with the coupling strength

In Poisson point process model, the coupling strength between two spike trains is determined by the proportion α. Given $d_P = 15\text{ms}$, two spike trains S_X and S_Y of 10s are generated. Spike train S_X drives spike train S_Y. The coupling strength α ranges from 0 to 1 with a step of 0.05. In Izhikevich's neuronal model, the parameter *R* which reflects the coupling strength ranges from 0 to 100% with a step of 5%. Spike trains for neuron 1 and neuron 2 are simulated with the causality from neuron 1 to neuron 2 and a delay time of 15ms. These spike trains are also of 10s length. As can be seen in Fig. 8(a) and 8(c), it is clear that the PCMI and TE are superior to the CE at identifying the coupling direction. As far as PCMI and TE are concerned, the advantage of the PCMI is that it can determine the coupling direction with more reliability and robustness for the weak coupling. Fig. 8(b) and 8(d) plot the PCMI values for different coupling strengths in each model. In the direction from S_X to S_Y (from neuron 1 to neuron 2), the PCMI estimate is proportional to $\alpha(R)$. On the other hand, the PCMI estimate is always close to 0 because there is no causality between two spike trains in the opposite direction.

(2) The effect of spike train duration on the directionality index estimation

Since the three methods for comparison in this study all depend on the statistical calculation, it is necessary to investigate the effect of the duration of spike trains on the directionality index estimation. In Poisson point process model, Given $d_P = 15\text{ms}$, two spike trains S_X and S_Y are generated with the driving direction from S_X to S_Y. Fig. 9(a) and 9(b) plot the directionality index estimated by the PCMI, TE and CE for two different coupling strength: $\alpha = 0.1$ and $\alpha = 0.3$. In Fig. 9(a), with the

increase of duration, the directionality index of PCMI increases with small fluctuations and then becomes stationary. In comparison, the directionality index of TE is not suitable for estimating the directionality index because of the large fluctuations and the small directionality index. As can be seen in Fig. 9(b), the behavior of PCMI and TE are similar, but the PCMI is still superior to the TE, especially when the spike trains duration is less than 10s. In both of the cases, compared with PCMI and TE, the directionality index of the CE does not change obviously with the spike train duration but it is not very efficient to evaluate the coupling detection. The effect of spike train duration on the PCMI values for the two coupling strengths are described in Fig. 9(c) and 9(d). It was found that that there is a significant decrease for $\alpha = 0.1$ ($I_{X\to Y}$ decreases form 0.003 to 0.001 and $I_{Y\to X}$ decreases from 0.001 to 0 for short durations), for other coupling strengths, the PCMI value almost does not vary with the spike train durations. The simulation results for Izhikevich's neuronal model are shown in Fig. 10. Neuron 1 drives neuron 2 with a delay time of 15ms. Two different coupling strength are selected as R = 10% and R = 30%. It can be observed similar results to the Poisson point process model.

(3) The robustness of directionality index

Three types of noise are considered in this study: the jitter noise corresponding to a shift in time of the spikes in spike trains; the missing spikes corresponding to the random deletion of spikes in spike trains; the extra spikes corresponding to the random insertion of independent spikes in spike trains. The jitter noise may appear in stochastic biological processes such as synaptic transmission and spike propagation in a neural network. The missing and extra spikes arise as spurious points in the spike trains, primarily caused by spikes which are not fired by the recorded neuron, but by other external processes involving the discharges of other neurons, errors in the spike sorting procedure, electrical artifacts, etc. [19, 63].

For the Poisson point process model, given $d_P = 15\text{ms}$, two spike trains S_X and S_Y of 10s duration are generated. Spike train S_X drives spike train S_Y. We investigate the effect of noise on the directionality index estimation in two cases: $\alpha = 0.1$ and $\alpha = 0.3$. For the Izhikevich's neuronal model, neuron 1 drives neuron 2 with a delay time of 15ms. The simulated spike trains are of 10s length. The effect of

noise on the directionality index estimation is evaluated by the models of two different coupling strengths: R = 10% and R = 30%.

(1) Jitter noise. The jitter noise is added to the spike trains via shifting every spike in each spike train by a time normally distributed in an interval. For the Poisson point process model, the performance of the three methods to estimate the coupling direction dramatically decreased with the increasing of the magnitude of the jitter noise, as illustrated in Fig. 11(a) and 11(b). For the coupling strength $\alpha = 0.1$, the PCMI and TE can resist the jitter noise only when the jitter is smaller than 10ms and the PCMI is prior to TE. But the CE cannot against the jitter noise. For the coupling strength $\alpha = 0.3$, the TE is a little more immune than the PCMI but only for the small jitter noise (< 20ms). The CE still can't overcome the effect of the jitter noise. In Fig. 11(c) and 11(d), the PCMI estimate from S_X to S_Y ($I_{X\to Y}$) is greatly influenced by the jitter noise which leads to the poor ability of identifying the coupling direction. From the simulation results for the Izhikevich's neuronal model which are shown in Fig. 12, it can be observed that the performance of PCMI and TE to resist jitter noise are very close to each other. However, they can only resist small jitter noise. The capability of CE method is almost similar to the Poisson point process model.

(2) Missing spikes. The amount of missing spikes is quantified by the percentage of randomly deleted spikes in each spike train. For the Poisson point process model, the simulation results for the directionality index are shown in Fig. 13(a) and 13(b). For the coupling strength $\alpha = 0.1$, the directionality index estimated by the PCMI decreases with the increasing number of missing spikes. The directionality index of TE fluctuates dramatically and the directionality index of CE stays around zero. For the coupling strength $\alpha = 0.3$, the effect of the missing spikes on the PCMI and CE are not significant, but the directionality index of TE decreases significantly. Fig. 13(c) and 13(d) plot the variation of PCMI values with the missing spikes. With the increasing of missing spikes, $I_{X\to Y}$ decreases significantly and $I_{Y\to X}$ increases very slightly. But $I_{X\to Y}$ is always lager than $I_{Y\to X}$ which ensures a correct estimation of the coupling direction. The simulation results for the Izhikevich's neuronal model are shown in Fig. 14. Clearly, the PCMI is still superior to the TE and CE. Although the performance of PCMI is deteriorated due to the missing spikes, it can tell the correct coupling direction between two neurons either for R = 10% or R = 30%.

(3) Extra spikes. The amount of extra spikes is quantified by the percentage of randomly inserted independent spikes in each spike train. With regard to the Poisson point process model, Fig. 15(a) and 15(b) show the estimation of directionality index by the PCMI, the TE and CE as a function of extra spikes. For the coupling strength $\alpha = 0.1$, the extra spikes make the directionality index of PCMI decrease to about 0.4 when the number of the extra noisy spikes is equal to the original spikes number. But the PCMI is still capable of estimating the coupling direction. On the other hand, the TE is not suitable for estimating the coupling direction due to its uncertain results and the CE is not appropriate because of its approximate zero values. For the coupling strength $\alpha = 0.3$, the directionality index of the TE and CE are both influenced severally by the extra spike noise. However, there is only a small decrease for the PCMI with the increasing of the noisy spikes. As can be seen in Fig. 15(c) and 15(d), there is variation of the PCMI values because of the extra spikes, but this does not alter the result about the coupling direction, which is similar to the case of missing spikes. In Fig. 16, the simulation results of the Izhikevich's neuronal model are illustrated. The decrease of PCMI value from neuron 1 to neuron 2 ($I_{1\to 2}$) and the increase of the value on the opposite direction ($I_{2\to 1}$) lead to the decrease of the directionality index, especially for the case of R = 10%. However, the PCMI is still superior to TE and CE at identifying the coupling direction between neurons.

IV. CONCLUSIONS

Characterizing the connections between individual neurons is essential for the better understanding of neural coding. In this study, the PCMI method is proposed to identify the causal relationships (information flow) between two spike trains. To assess the performance of the measure, a series of simulations were performed by means of the Poisson point process model and Izhikevich's neuronal model. The simulation results shows that the PCMI method can be applied for the analysis of causality between neurons by spike trains. In comparison with the TE and CE methods, the advantages of the PCMI can be summarized in the following. (1) The PCMI can detect the interaction delays between two spike trains, even if there is a wide distribution of the delay times due to the multiple pathways that connect two neurons. The interaction delays are indicated by the product of δ and Δ and the

resolution is determined by Δ. (2) The PCMI method is able to estimate the directionality index reliably for the weak coupling strength (e.g. $\alpha = 0.1$ for Poisson point process model and R = 10% for Izhikevich's neuronal model) between spike trains, but the TE and CE methods are not suitable in this case because of the dramatically fluctuations and small values of the directionality index, respectively. For the stronger coupling strength (e.g. $\alpha = 0.3$ for Poisson point process model and R = 30% for Izhikevich's neuronal model), the three methods are able to identify the directionality index, but the PCMI is better than the TE and CE at identifying the coupling direction for short spike trains. (3) The PCMI is more robust to the noise in spike trains than the TE and CE, particularly for the missing and extra spikes. The underlying reason is that the PCMI is based on the ordinal patterns contained in the spike trains, thus the missing or extra spikes cannot severely destroy the inherent ordinal patterns, particularly when there is a stronger coupling strength between two spike trains. On the other hand, because the TE is calculated in terms of the number of spikes in time intervals and the CE is computed by means of the relative inter-spike intervals between a pair of spike trains, therefore they are influenced greatly by the missing and extra spikes. In summary, the PCMI method can give the quantification of the directionality index and the detection of temporal dynamics between two interacting spike trains.

However, there are two points should be noted in the application of the PCMI method. The first one is the robustness of the PCMI against the jitter noises. Another is whether the PCMI method can be used to estimate the information flow in multiple spike trains. These two issues will be investigated in future studies.

ACKNOWLEDGMENTS

This research was partly supported by National Natural Science Foundation of China (61025019, 90820016) and Natural Science Foundation of Hebei China (F2009001638).

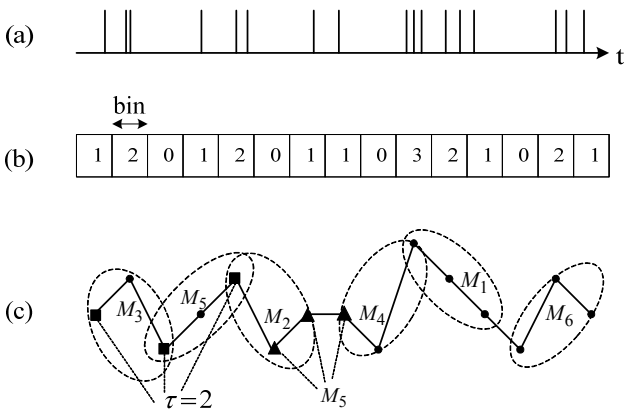

FIG. 1. Extraction of motifs from a simulated spike train. (a) A simulated spike train. (b) Discretize the spike train by adding spikes in each bin. (c) Motifs contained in the discretized sequence (order: m=3, so 3!=6 different motifs), including 'slopes' (M_1 and M_5), 'peaks' (M_2 and M_4) and 'troughs' (M_3 and M_6). The numbers indicate six different motifs which are defined identical to Li and Ouyang [48].

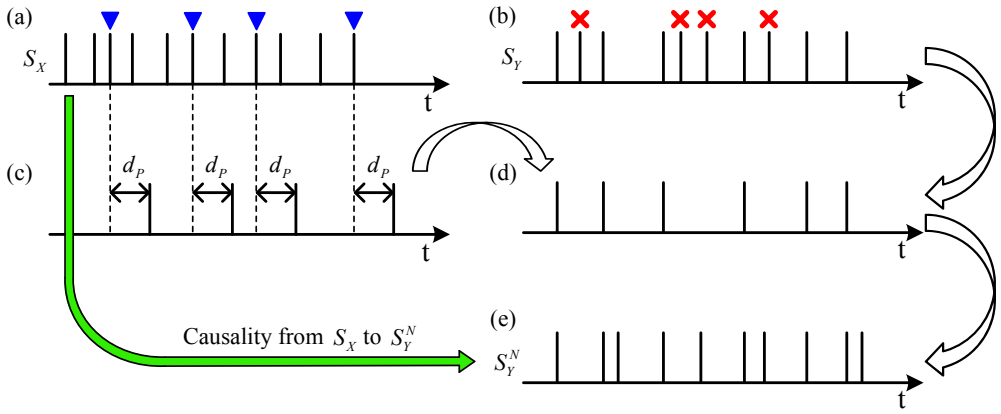

FIG.2. (Color online) Approach to construct causality between spike trains for Poisson point process model. (a) and (b) Two independent spike trains S_X and S_Y. The forks denote the randomly removed spikes from S_Y. The triangles denote the randomly selected spikes from S_X. (c) The spikes selected from S_X are delayed by d_P. (d) The remain spikes of S_Y. (e) The new spike train which contains the causal information of S_X.

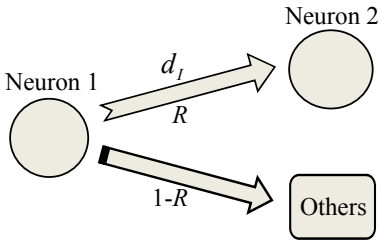

Fig. 3. Two coupled neurons for Izhikevich's neuronal model. Neuron 1 drives neuron 2 with a time delay which is denoted by d_1. The coupling strength is qualified by R which means the proportion of the output of neuron 1 injected into neuron 2.

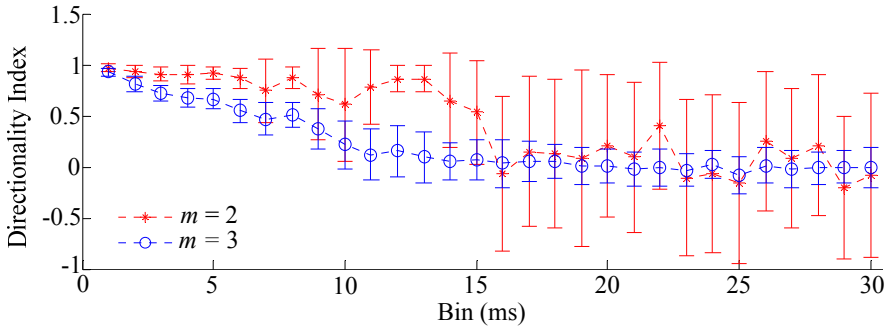

FIG. 4. (Color online) Directionality indexes for different bins which are given in mean ± SD (20 realizations for each order).

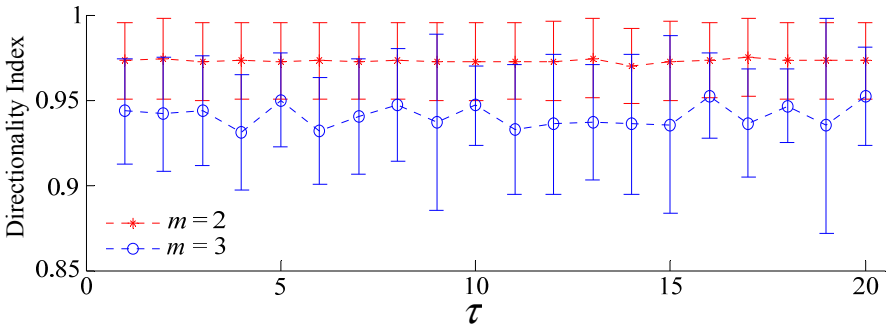

FIG. 5. (Color online) Directionality indexes for different lags which are given in mean ± SD (20 realizations for each order).

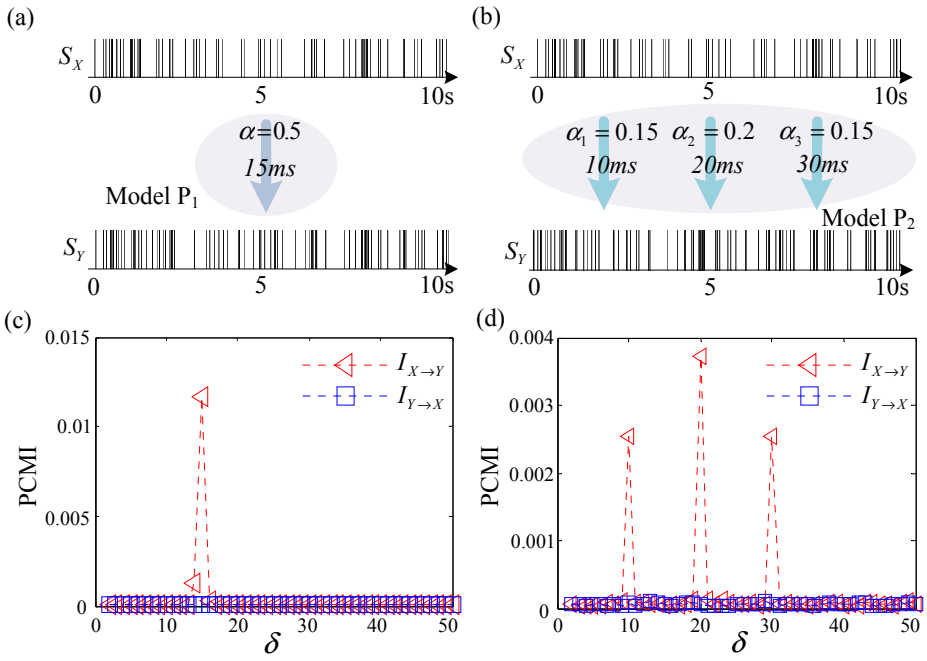

FIG. 6. (Color online) The PCMI estimate for Poisson point process models. (a) Model P_1: one delay of 15ms between S_X and S_Y, 0.5 of spikes in S_Y are borrowed from S_X. (b) Model P_2: three different delays of 10ms, 20ms and 30ms between S_X and S_Y, 0.15, 0.2 and 0.15 of spikes associated with each delay in S_Y are borrowed from S_X. (c) and (d) The PCMI estimate between S_X and S_Y ($I_{X\to Y}$ and $I_{Y\to X}$) with different δ values for model P_1 and model P_2.

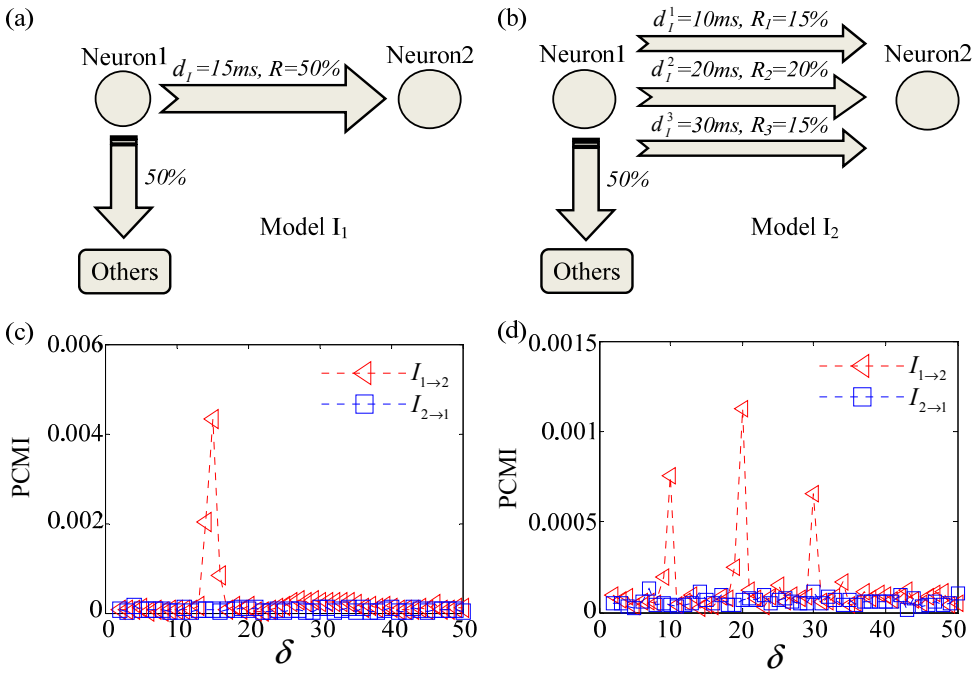

FIG. 7. (Color online) The PCMI estimate for Izhikevich's neuronal models. (a) Model I_1: one delay of 15ms between neuron 1 and neuron 2, 50% of the output of neuron 1 is injected into neuron 2. (b) Model I_2: three different delays of 10ms, 20ms and 30ms between neuron 1 and neuron 2, 15%, 20% and 15% of the output of neuron 1 associated each delay is injected into neuron 2. (c) and (d) The PCMI estimate between neuron 1 and neuron 2 ($I_{1\to2}$ and $I_{2\to1}$) with different δ values for model I_1 and model I_2.

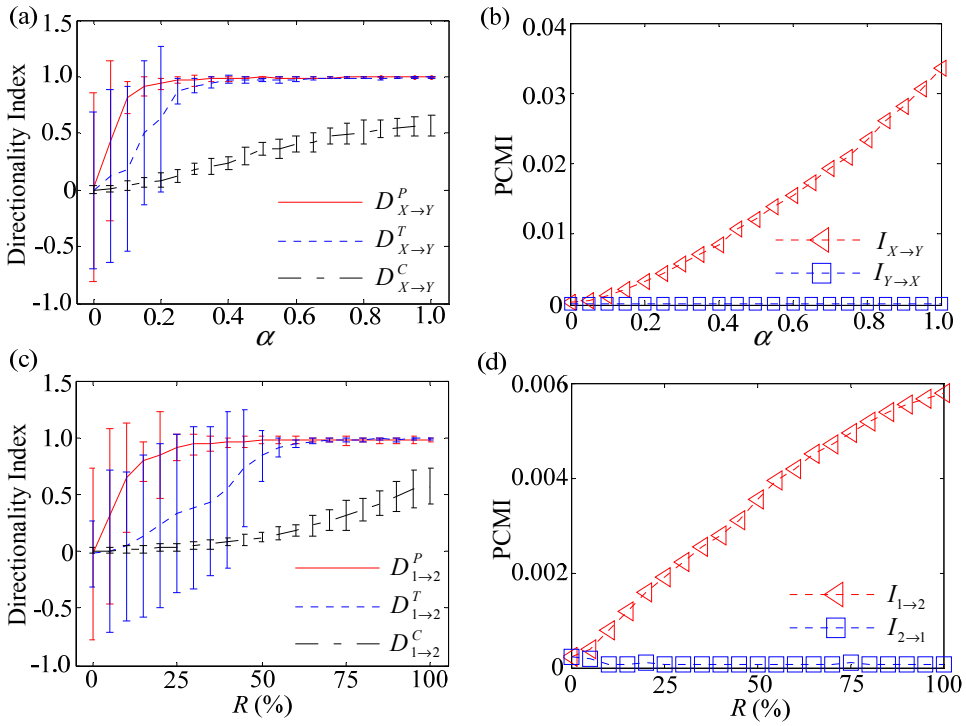

FIG. 8. (Color online) Directionality index and PCMI values for different coupling strength. (a) and (c) Directionality index estimated by PCMI, TE and CE for Poisson point process model ($D^P_{X\to Y}$, $D^T_{X\to Y}$ and $D^C_{X\to Y}$) and Izhikevich's neuronal model ($D^P_{1\to 2}$, $D^T_{1\to 2}$ and $D^C_{1\to 2}$), respectively. The results are given in the form of mean$\pm$SD (20 realizations for each method). (b) and (d) PCMI values for different coupling strength. $I_{X\to Y}$ and $I_{Y\to X}$ for Poisson point process model, $I_{1\to 2}$ and $I_{2\to 1}$ for Izhikevich's neuronal model.

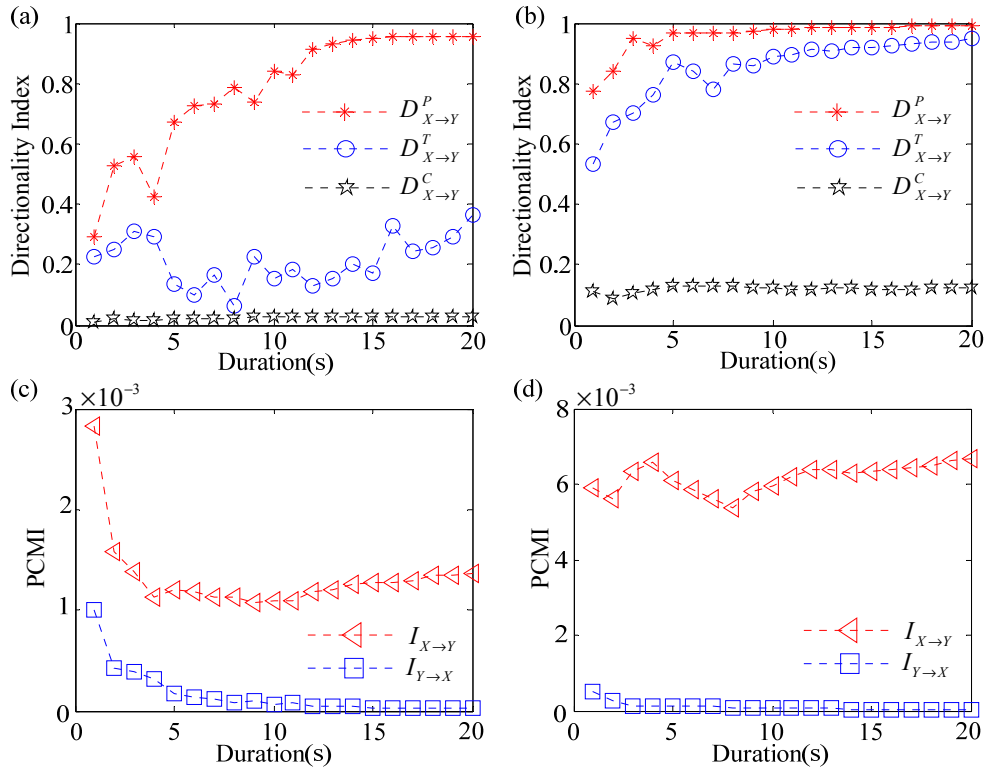

FIG. 9. (Color online) Effect of spike train duration on the directionality index and PCMI values for Poisson point process model. (a) and (b) Directionality index estimated by the PCMI, TE and CE ($D^P_{X\to Y}$, $D^T_{X\to Y}$ and $D^C_{X\to Y}$) for $\alpha = 0.1$ and $\alpha = 0.3$. (c) and (d) PCMI values ($I_{X\to Y}$ and $I_{Y\to X}$) with different durations for $\alpha = 0.1$ and $\alpha = 0.3$.

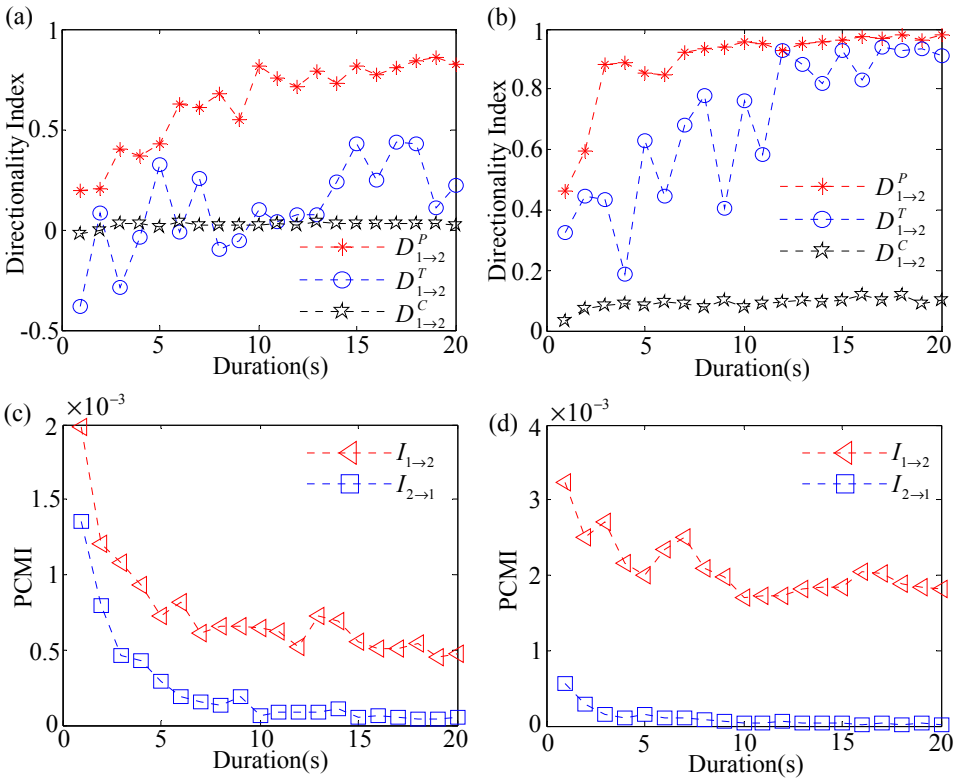

FIG. 10. (Color online) Effect of spike train duration on the directionality index and PCMI values for Izhikevich's neuronal model. (a) and (b) Directionality index estimated by the PCMI, TE and CE ($D^P_{1\to2}$, $D^T_{1\to2}$ and $D^C_{1\to2}$) for R = 10% and R = 30%. (c) and (d) PCMI values ($I_{1\to2}$ and $I_{2\to1}$) with different durations for R = 10% and R = 30%.

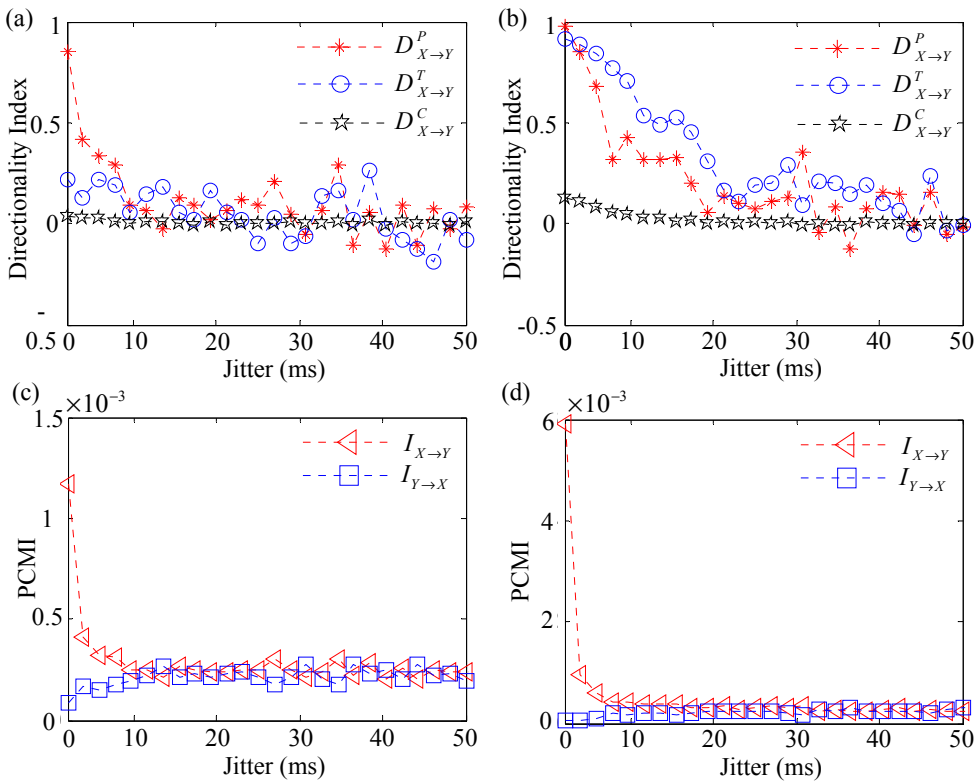

FIG. 11. (Color online) Effect of jitter noise on the directionality index and PCMI values for Poisson point process model. (a) and (b) The robustness of directionality index estimated by the PCMI, TE and CE ($D^P_{X\to Y}$, $D^T_{X\to Y}$ and $D^C_{X\to Y}$) against jitter noise for $\alpha = 0.1$ and $\alpha = 0.3$. (c) and (d) The variation of PCMI values ($I_{X\to Y}$ and $I_{Y\to X}$) with different jitters for $\alpha = 0.1$ and $\alpha = 0.3$.

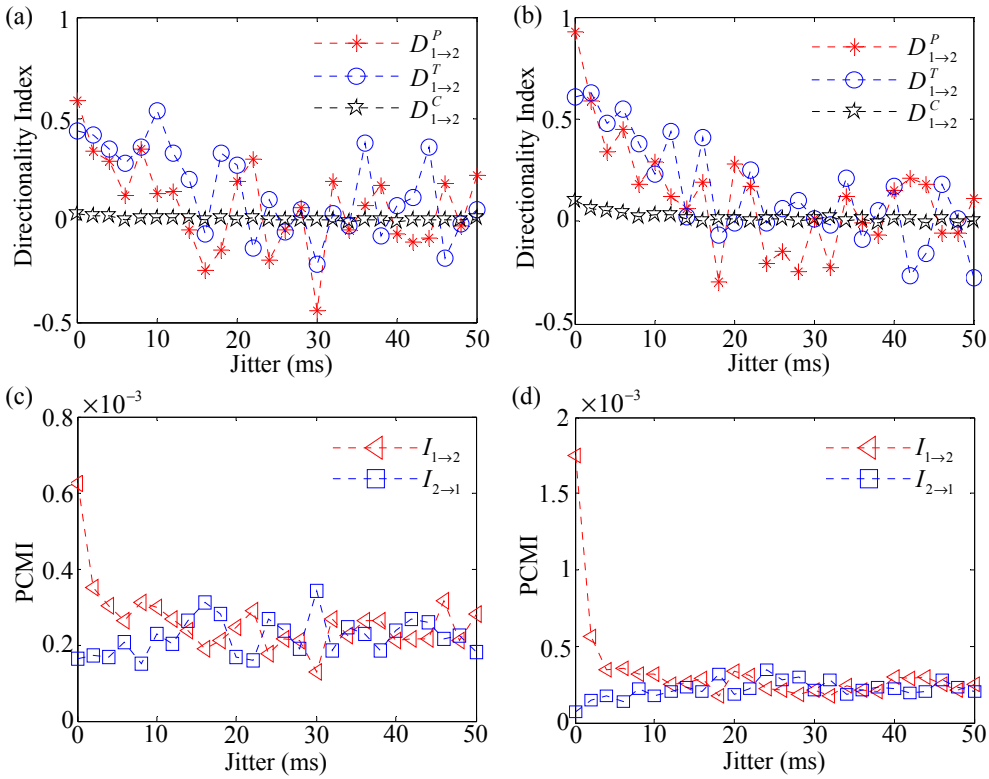

FIG. 12. (Color online) Effect of jitter noise on the directionality index and PCMI values for Izhikevich's neuronal model. (a) and (b) The robustness of directionality index estimated by the PCMI, TE and CE ($D^P_{1\to2}$, $D^T_{1\to2}$ and $D^C_{1\to2}$) against jitter noise for R = 10% and R = 30%. (c) and (d) The variation of PCMI values ($I_{1\to2}$ and $I_{2\to1}$) with different jitters for R = 10% and R = 30%.

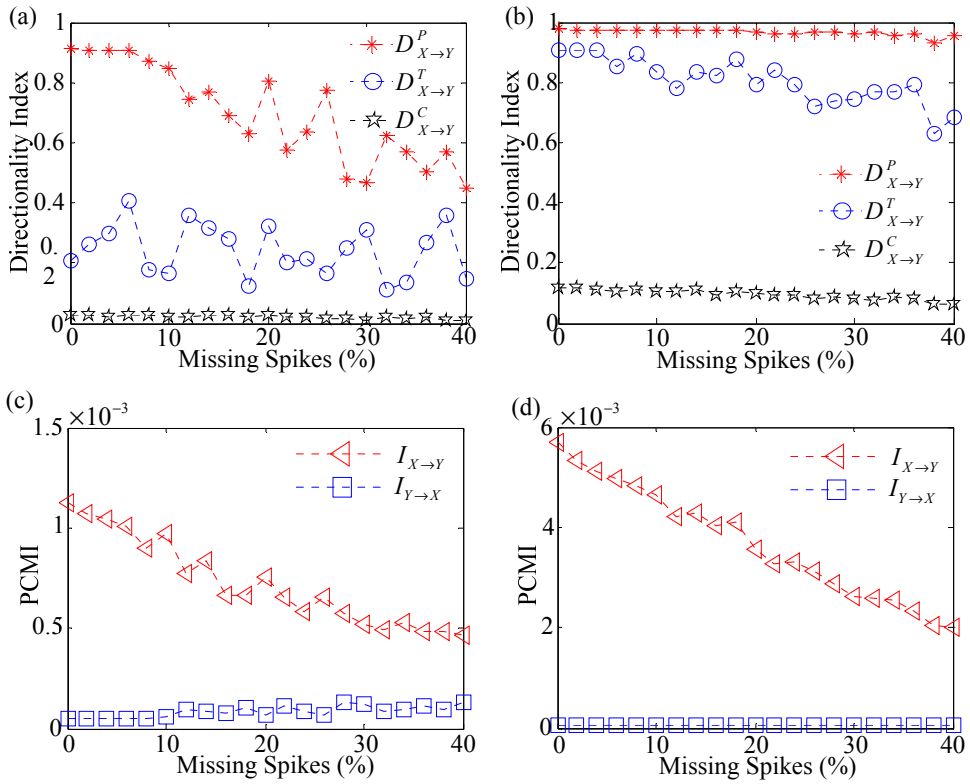

FIG. 13. (Color online) Effect of missing spikes on the directionality index and PCMI values for Poisson point process model. (a) and (b) The robustness of directionality index estimated by the PCMI, TE and CE ($D^P_{X\to Y}$, $D^T_{X\to Y}$ and $D^C_{X\to Y}$) against missing spikes for $\alpha = 0.1$ and $\alpha = 0.3$. (c) and (d) The variation of PCMI values ($I_{X\to Y}$ and $I_{Y\to X}$) with different percentage of missing spikes for $\alpha = 0.1$ and $\alpha = 0.3$.

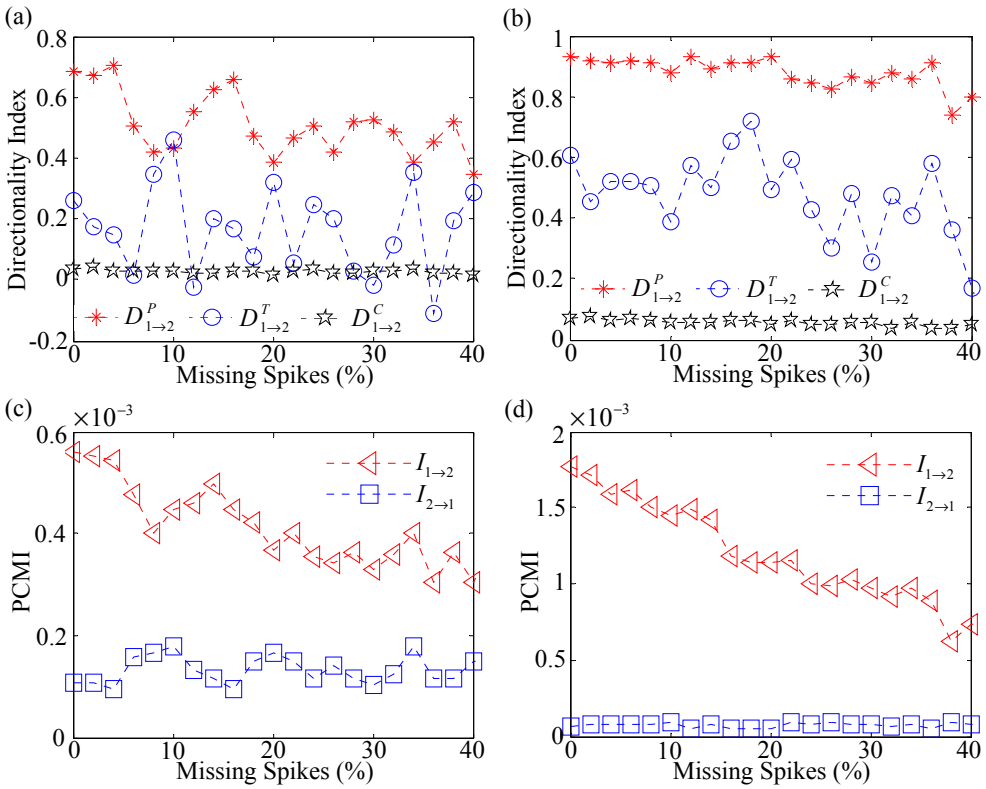

FIG. 14. (Color online) Effect of missing spikes on the directionality index and PCMI values for Izhikevich's neuronal model. (a) and (b) The robustness of directionality index estimated by the PCMI, TE and CE ($D^P_{1\to2}$, $D^T_{1\to2}$ and $D^C_{1\to2}$) against jitter noise for R = 10% and R = 30%. (c) and (d) The variation of PCMI values ($I_{1\to2}$ and $I_{2\to1}$) with different jitters for R = 10% and R = 30%.

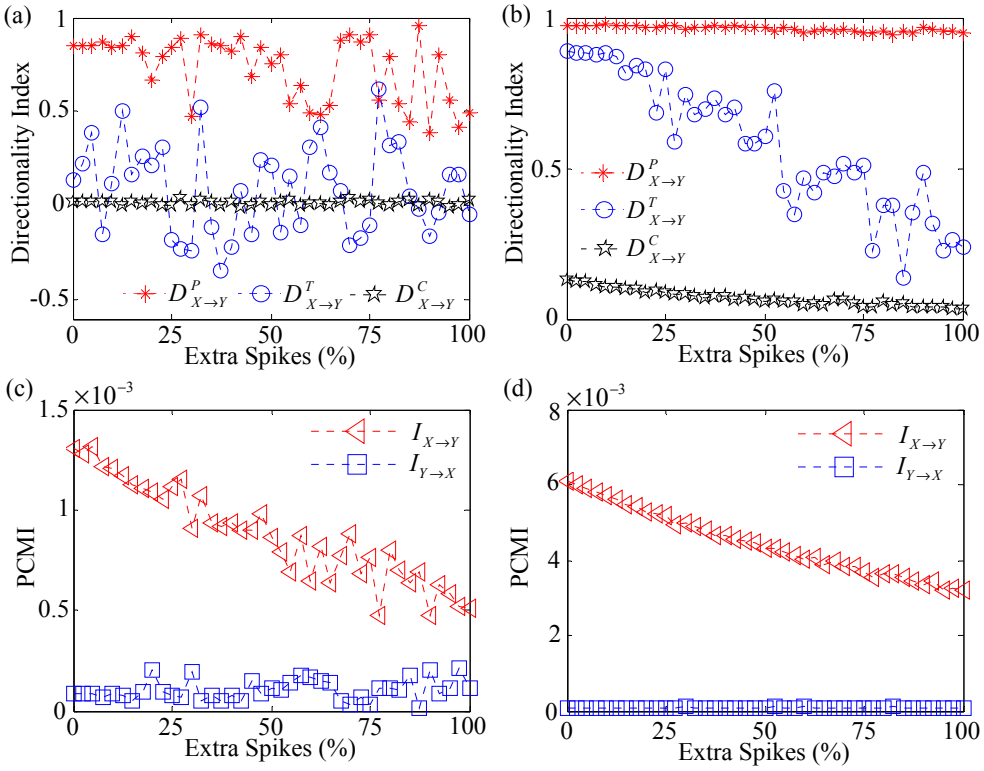

FIG. 15. (Color online) Effect of extra spikes on the directionality index and PCMI values for Poisson point process model. (a) and (b) The robustness of directionality index estimated by the PCMI, TE and CE ($D^P_{X\to Y}$, $D^T_{X\to Y}$ and $D^C_{X\to Y}$) against extra spikes for $\alpha = 0.1$ and $\alpha = 0.3$. (c) and (d) The variation of PCMI values ($I_{X\to Y}$ and $I_{Y\to X}$) with different percentage of extra spikes for $\alpha = 0.1$ and $\alpha = 0.3$.

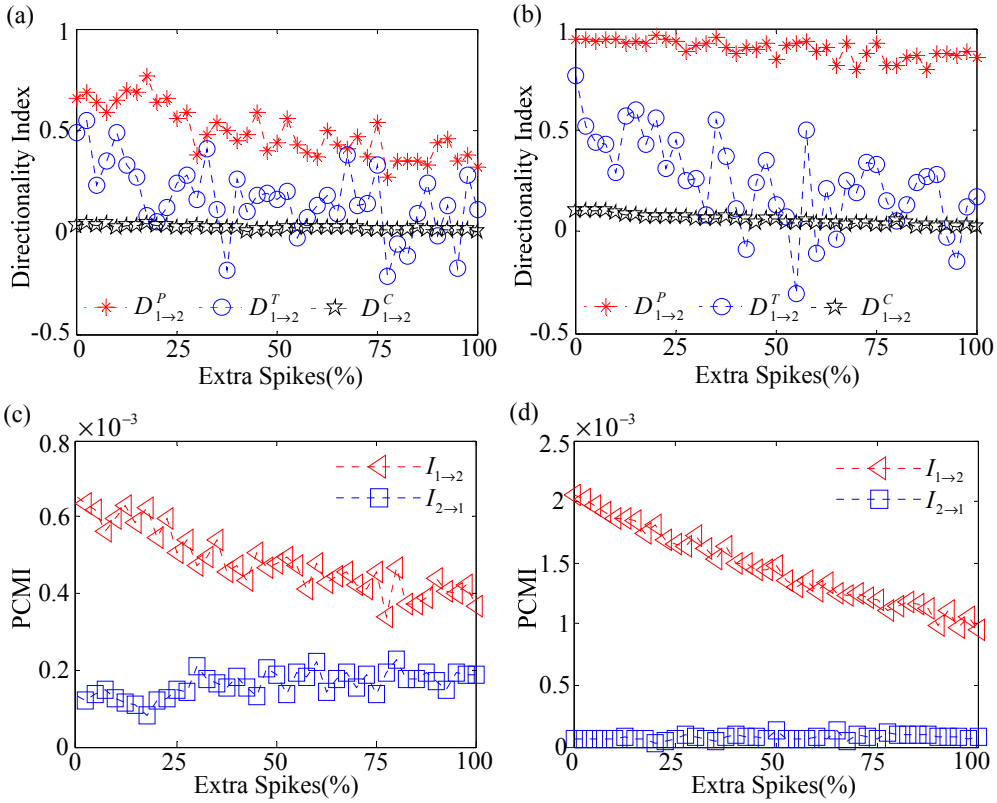

FIG. 16. (Color online) Effect of extra spikes on the directionality index and PCMI values for Izhikevich's neuronal model. (a) and (b) The robustness of directionality index estimated by the PCMI, TE and CE ($D^P_{1\to2}$, $D^T_{1\to2}$ and $D^C_{1\to2}$) against jitter noise for R = 10% and R = 30%. (c) and (d) The variation of PCMI values ($I_{1\to2}$ and $I_{2\to1}$) with different jitters for R = 10% and R = 30%.

References

[1] A. Pouget, P. Dayan, and R. Zemel, Nat Rev Neurosci **1**, 125 (2000).

[2] R. C. deCharms, and A. Zador, Annu Rev Neurosci **23**, 613 (2000).

[3] I. Nemenman *et al.*, PLoS Comput Biol **4**, e1000025 (2008).

[4] I. E. Ohiorhenuan *et al.*, Nature **466**, 617 (2010).

[5] B. B. Averbeck, P. E. Latham, and A. Pouget, Nat Rev Neurosci **7**, 358 (2006).

[6] B. Cessac, H. Paugam-Moisy, and T. Viéville, Journal of Physiology-Paris **104**, 5 (2010).

[7] A. S. Dickey *et al.*, J Neurophysiol **102**, 1331 (2009).

[8] V. Kandagor *et al.*, Conf Proc IEEE Eng Med Biol Soc **1**, 6243 (2010).

[9] P. Fries *et al.*, Nat Neurosci **4**, 194 (2001).

[10] M. Zochowski *et al.*, J Neurosci **20**, 8485 (2000).

[11] T. Sasaki *et al.*, J Physiol **574**, 195 (2006).

[12] N. Takahashi *et al.*, Neuroscience Research **58**, 219 (2007).

[13] E. Brown, R. Kass, and P. Mitra, Nature Neuroscience **7**, 456 (2004).

[14] E. Salinas, and T. Sejnowski, Nat Rev Neurosci **2**, 539 (2001).

[15] J. D. Victor, and K. P. Purpura, J Neurophysiol **76**, 1310 (1996).

[16] J. Victor, and K. Purpura, Netw Comput Neural Syst **8**, 127 (1997).

[17] M. C. van Rossum, Neural Comput **13**, 751 (2001).

[18] J. S. Haas, and J. A. White, J Neurophysiol **88**, 2422 (2002).

[19] S. Schreiber *et al.*, Neurocomputing **52-54**, 925 (2003).

[20] R. Quian Quiroga, T. Kreuz, and P. Grassberger, Phys. Rev. E **66**, 041904 (2002).

[21] T. Kreuz *et al.*, Journal of Neuroscience Methods **165**, 151 (2007).

[22] R. Narayan, G. Grana, and K. Sen, J Neurophysiol **96**, 252 (2006).

[23] J. M. Fellous *et al.*, J Neurosci **24**, 2989 (2004).

[24] L. Wang *et al.*, J Neurosci **27**, 582 (2007).

[25] Y. Chen *et al.*, Phys Lett A **324**, 26 (2004).

[26] A. K. Seth, Network **16**, 35 (2005).

[27] M. Ding, Y. Chen, and S. Bressler, Handbook of Time Series Analysis (Wiley, 2006).

[28] A. K. Seth, Journal of Neuroscience Methods **186**, 262 (2010).

[29] M. Kamiński *et al.*, Biological Cybernetics **85**, 145 (2001).

[30] M. Havlicek *et al.*, NeuroImage **53**, 65 (2010).

[31] A. G. Nedungadi *et al.*, J Comput Neurosci **27**, 55 (2009).

[32] M. Krumin, and S. Shoham, Comput Intell Neurosci, 752428 (2010).

[33] M. Palu, and A. Stefanovska, Phys. Rev. E **67**, 55201 (2003).

[34] M. Palu *et al.*, Phys. Rev. E **63**, 46211 (2001).

[35] R. Vicente *et al.*, J Comput Neurosci **30**, 45 (2011).

[36] T. Schreiber, Phys. Rev. Lett. **85**, 461 (2000).

[37] C. Bandt, and B. Pompe, Phys. Rev. Lett. **88**, 174102 (2002).

[38] E. Olofsen, J. W. Sleigh, and A. Dahan, Br J Anaesth **101**, 810 (2008).

[39] K. Hlavkov Schindler *et al.*, Phys Rep **441**, 1 (2007).

[40] J. Waddell *et al.*, Journal of Neuroscience Methods **162**, 320 (2007).

[41] B. Gourévitch, and J. Eggermont, J Neurophysiol **97**, 2533 (2007).

[42] D. Li *et al.*, J Neural Eng **7**, 046010 (2010).

[43] X. Li, G. Ouyang, and D. A. Richards, Epilepsy Res **77**, 70 (2007).

[44] X. Li, S. Cui, and L. J. Voss, Anesthesiology **109**, 448 (2008).

[45] M. Vejmelka, and M. Palus, Phys. Rev. E **77**, 026214 (2008).

[46] R. Salvador *et al.*, Front Neuroinformatics **4**, 115 (2010).

[47] A. Bahraminasab *et al.*, Phys. Rev. Lett. **100**, 84101 (2008).

[48] X. Li, and G. Ouyang, NeuroImage **52**, 497 (2010).

[49] R. Dzakpasu, and M. Zochowski, Physica D **208**, 115 (2005).

[50] J. Shlens *et al.*, Neural Comput **19**, 1683 (2007).

[51] S. Strong *et al.*, Phys. Rev. Lett. **80**, 197 (1998).

[52] J. Thomas, and T. Cover, *Elements of information theory* (Wiley-Interscience, 1991).

[53] M. G. Rosenblum *et al.*, Phys. Rev. E **65**, 041909 (2002).

[54] J. W. Schnupp *et al.*, J Neurosci **26**, 4785 (2006).

[55] See Supplemental Material at [URL will be inserted by publisher] for the matlab codes of the algorithm.

[56] W. J. Ma *et al.*, Nat Neurosci **9**, 1432 (2006).

[57] M. E. Mazurek, and M. N. Shadlen, Nat Neurosci **5**, 463 (2002).

[58] E. M. Izhikevich, IEEE Trans Neural Netw **14**, 1569 (2003).

[59] S. Feldt *et al.*, Phys. Rev. E **79**, 056104 (2009).

[60] M. Merkel, and B. Lindner, Phys. Rev. E **81**, 041921 (2010).

[61] M. Shelhamer, *Nonlinear dynamics in physiology: a state-space approach* (World Scientific Pub Co Inc, 2007).

[62] H. A. Swadlow, D. L. Rosene, and S. G. Waxman, Exp Brain Res **33**, 455 (1978).

[63] Y. Asai, and A. E. Villa, J Biol Phys **34**, 325 (2008).